INTERNATIONAL JOURNAL FOR NUMERICAL AND ANALYTICAL METHODS IN GEOMECHANICS
Int. J. Numer. Anal. Meth. Geomech. (2014)
Published online in Wiley Online Library (wileyonlinelibrary.com). DOI: 10.1002/nag.2250

A finite strain closed-form solution for the elastoplastic ground response curve in tunnelling

Apostolos Vrakas*,† and Georgios Anagnostou

ETH Zurich, Switzerland

SUMMARY

The ground response to tunnel excavation is usually described in terms of the characteristic line of the ground (also called 'ground response curve', GRC), which relates the support pressure to the displacement of the tunnel wall. Under heavily squeezing conditions, very large convergences may take place, sometimes exceeding 10–20% of the excavated tunnel radius, whereas most of the existing formulations for the GRC are based on the infinitesimal deformation theory. This paper presents an exact closed-form analytical solution for the ground response around cylindrical and spherical openings unloaded from isotropic and uniform stress states, incorporating finite deformations and linearly elastic-perfectly plastic rock behaviour obeying the Mohr–Coulomb failure criterion with a non-associated flow rule. Additionally, the influence of out-of-plane stress in the case of cylindrical cavities under plane-strain conditions is examined. The solution is presented in the form of dimensionless design charts covering the practically relevant parameter range. Finally, an application example is included with reference to a section of the Gotthard Base tunnel crossing heavily squeezing ground. The expressions derived can be used for preliminary convergence assessments and as valuable benchmarks for finite strain numerical analyses. Copyright © 2014 John Wiley & Sons, Ltd.

Received 1 August 2013; Revised 9 November 2013; Accepted 15 November 2013

KEY WORDS: cavity contraction; closed-form solution; ground response curve; large strains; Mohr–Coulomb; tunnels

1. INTRODUCTION

The so-called 'ground response curve' (GRC) shows the relationship between the support pressure and the displacement of the wall of a cylindrical tunnel under rotationally symmetric conditions. It is widely used for studying (i) the response of the ground to tunnel excavation and (ii) its interaction with the tunnel support (the so-called convergence–confinement method, Panet [1]). Apart from tunnelling (the primary focus of the current study), the problem of cavity contraction in elastoplastic rocks or soils may also be of great interest in mining (e.g. shaft design) and petroleum (e.g. borehole drilling) engineering.

The majority of existing analytical solutions concerning the GRC are based on the infinitesimal deformation theory and take account of several elastoplastic or even elastoviscoplastic constitutive models. (A concise review of existing solutions up to the early 80s was presented by Brown *et al*. [2], and further lists have been provided by Yu [3] and Alonso *et al*. [4]). However, large convergences are often encountered in underground projects combining high overburden with poor ground properties. Several case studies are to be found in the literature dealing with tunnelling under squeezing conditions, including for the Gotthard Base tunnel in Switzerland (Kovári *et al*. [5]), and Kovári [6], Hoek [7] and Barla [8] have presented comprehensive reviews on the topic. It is known that the excavation technique and the support measures greatly affect the stability of the excavation

*Correspondence to: Apostolos Vrakas, ETH Zurich, Switzerland, Wolfgang-Pauli-Strasse 15, 8093 Zurich, Switzerland.
†E-mail: apostolos.vrakas@igt.baug.ethz.ch

area, especially under squeezing conditions. Nevertheless, wall displacements exceeded one tenth of the radius initially excavated in many reported cases, sometimes despite the prompt installation of temporary supports (Figure 1), and have even resulted in a total closure of the opening, for instance at the Yacambú-Quibor tunnel in Venezuela (Hoek [7]).

In such cases, the applicability of the classic formulation based on infinitesimal deformations is questionable. Although a consideration of both equilibrium and stiffness on the deformed (or current) configuration (Figure 2b) instead of the undeformed (or initial) one (Figure 2a) seems more appropriate for an assessment of the ground behaviour around an underground opening, few attempts have been made to derive a robust solution to the GRC based on large strain theory. Papanastasiou and Durban [9] studied the problems of both expanding (internally pressurized) and contracting (externally pressurized) cylindrical cavities in an infinite isotropic medium using the Mohr–Coulomb (MC) and the Drucker–Prager hardening solids, resulting in differential equations which had to be solved numerically. Later, Yu and Rowe [10] presented an analytical solution to the problem of cavity wall unloading (for both cylindrical and spherical symmetry) using the linearly elastic-perfectly plastic MC model. However, they ignored elastic deformations within the plastic zone in order to express the cavity contraction curve in closed form. On the other hand, the problem of cavity expansion, which is of great interest in geotechnical engineering due to its wide application (cf. the interpretation of pressuremeter and penetrometer tests, the installation of driven piles, etc.), has been studied thoroughly within the framework of finite deformations. Yu [3] has summarized several significant analytical solutions for cavity problems based on both small and large strain formulations in combination with various failure criteria. It is worth mentioning here, for the sake of completeness, the recent exact finite strain solution, provided by Chen and Abousleiman [11], with respect to soil-like materials that obey the modified Cam-clay constitutive model. The solution can be applied to the cavity contraction problem after some modifications, but cannot be expressed in closed form and thus numerical techniques are necessary.

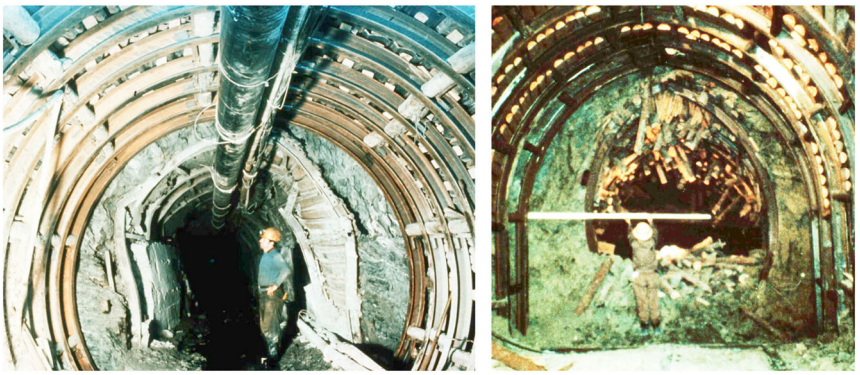

(a) (b)

Figure 1. Examples of very large deformations problems in tunnelling through squeezing ground: (a) Safety gallery of the Gotthard motorway tunnel, Switzerland; (b) Nakayama tunnel, Japan.

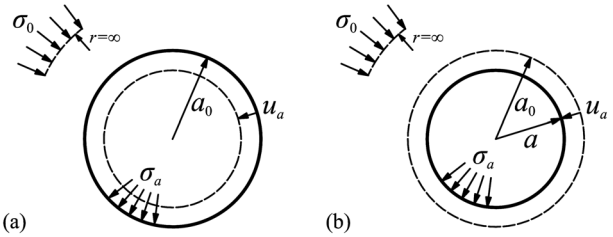

Figure 2. Problem setup for the determination of the GRC: (a) small strain approach; (b) large strain approach.

DOI: 10.1002/nag

In this paper, we present an explicit solution for the finite strain GRC which takes into account the unloading of cylindrical or spherical openings in an infinite linearly elastic, perfectly plastic medium obeying the MC yield criterion with a non-associated flow rule. (The spherical cavity problem is particularly relevant as an approximation of the problem of tunnel face extrusion in deep excavations – cf. Egger [12], Labiouse [13] and Mair [14]). The overall analysis is based on a (Total) Lagrangian approach observing the movement of each material point. After deriving the solution, we examine the influence of the out-of-plane plastic flow, which may occur around a cylindrical cavity under plane-strain conditions, and show that it can be neglected. Furthermore, we compare the predictions of the exact model presented with the small strain solution (Panet [1], Reed [15]) as well as with Yu and Rowe's [10] approximate large strain solution. Finally, we show the practical usefulness of the proposed large strain solution by means of an application example concerning a heavily squeezing section of the Gotthard Base tunnel in Switzerland.

2. PROBLEM STATEMENT

The present study concerns cases with atmospheric pore pressure, i.e. dry or completely drained grounds, where the influence of water is negligible. The cylindrical cavity problem is analysed together with the spherical one by introducing a variable ζ, which is equal to 1 or 2, respectively. This simultaneous treatment of the two and the three dimensional problem has been implemented by several researchers in the past; cf. inter alia Bigoni and Laudiero [16], Yu and Houlsby [17] and Yu and Rowe [10]. Cylindrical (r, t, z) and polar (r, $t \equiv z$) coordinates are used, respectively, for the formulation of the mathematical equations, with the axes origin being placed at the centre of the cavity. Plane-strain conditions are considered in the z direction for the cylindrical problem, while no distinction is made between the tangential directions in the case of spherical symmetry, implying that the corresponding stresses and strains remain equal throughout the analysis, i.e. the stress component $\sigma_z = \sigma_t$ and the strain component $\varepsilon_z = \varepsilon_t$.

The ground is considered to be homogeneous, isotropic and linearly elastic-perfectly plastic according to the MC failure criterion, which can be expressed as

$$\sigma_1 = m\sigma_3 + \sigma_D, \tag{1}$$

where

$$m = \frac{1 + \sin\varphi}{1 - \sin\varphi}. \tag{2}$$

The symbols σ_1, σ_3 and φ denote the maximum principal stress, the minimum principal stress and the friction angle, respectively. The uniaxial compressive strength σ_D is equal to

$$\sigma_D = \frac{2c\cos\varphi}{1 - \sin\varphi}, \tag{3}$$

where c denotes the cohesion. Stresses and strains are defined as positive in the case of compression.

The initial stress field is taken to be isotropic and uniform, i.e. $\sigma_r = \sigma_t = \sigma_z = \sigma_0$, where σ_r, σ_t and σ_z are the radial, tangential and axial (in the case of a cylindrical cavity) stresses, correspondingly. The assumption of a uniform initial stress field means that the body forces are neglected, allowing for a one-dimensional description of the problem in terms of the radial displacement u, whereas the above mentioned stresses are principal throughout the unloading, which facilitates the derivation of closed-form analytical solutions.

The support pressure σ_a decreases gradually, starting from its initial value which is equal to σ_0, whereas the stresses in the far field (theoretically, at an infinite distance from the opening) remain unaltered by the excavation. The boundary conditions then read as follows:

DOI: 10.1002/nag

$$\sigma_r(a) = \sigma_a, \tag{4}$$

$$\lim_{r\to\infty} \sigma_r(r) = \lim_{r\to\infty} \sigma_t(r) = \sigma_0. \tag{5}$$

Note that Eq. (4) applies to the deformed state. During the unloading of the excavation boundary, the cavity radius decreases from its initial value a_0 to the current radius a (Figure 2b), while a material point having the initial position r_0 (Lagrangian or material coordinate) is now at the current radius r (Eulerian or spatial coordinate). The radial displacement u of each material point is then defined as

$$u(r) = r_0 - r, \tag{6}$$

implying that is positive for contraction of the tunnel wall.

3. EQUILIBRIUM AND KINEMATIC RELATIONSHIPS

The stress equilibrium requirement in the current (deformed) state reads as follows:

$$\frac{d\sigma_r}{dr} + \zeta \frac{\sigma_r - \sigma_t}{r} = 0. \tag{7}$$

It should be noted that the stresses correspond to the Cauchy (or true) ones, acting on the current area of each infinitesimal element.

For the present type of problem, where no rotation of the principal axes takes place, Chadwick [18] proposed the use of logarithmic (or Hencky) strains, which according to the adopted sign conventions can be written in Eulerian form as follows:

$$\varepsilon_r = \ln\left(1 + \frac{du}{dr}\right) = \frac{du}{dr} - \frac{1}{2}\left(\frac{du}{dr}\right)^2 + \ldots, \tag{8}$$

$$\varepsilon_t = \ln\left(1 + \frac{u}{r}\right) = \frac{u}{r} - \frac{1}{2}\left(\frac{u}{r}\right)^2 + \ldots \tag{9}$$

In a small strain formulation, the higher order terms on the right side would be neglected, thus leading to the known kinematic equations.

4. DERIVATION FOR ELASTIC BEHAVIOUR

Initially, the response of the ground due to the decrease in support pressure at $r = a$ is purely elastic (Figure 3a). The solution to the current problem can be found in numerous studies, see for example Yu and Houlsby [17] or Yu and Rowe [10]. However, it is instructive to reproduce it here briefly in order to ensure the smooth flow of the forthcoming mathematical operations. Hooke's law can be written in incremental form as:

$$d\varepsilon_r^{EL} = \frac{1+v}{E}\left[\frac{1-(2-\zeta)v}{1+(\zeta-1)v} d\sigma_r - \frac{\zeta v}{1+(\zeta-1)v} d\sigma_t\right], \tag{10}$$

$$d\varepsilon_t^{EL} = \frac{1+v}{E}\left[\frac{1-v}{1+(\zeta-1)v} d\sigma_t - \frac{v}{1+(\zeta-1)v} d\sigma_r\right], \tag{11}$$

where ε_r and ε_t denote the radial and tangential strain, respectively, E is the Young's modulus and v represents the Poisson's ratio. In the case of the cylindrical cavity problem, the plane-strain constraint leads to

DOI: 10.1002/nag

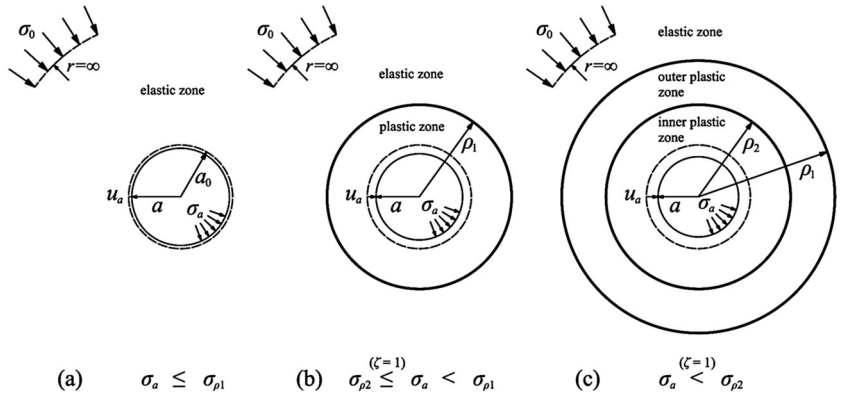

Figure 3. Behaviour of an unloaded cavity: (a) purely elastic response; (b) elastoplastic response (without or before out-of-plane plastic flow in the case of a cylindrical cavity); (c) elastoplastic response of a cylindrical cavity with out-of-plane plastic flow.

$$d\sigma_z = \nu(d\sigma_r + d\sigma_t), \tag{12}$$

which, after integration accounting for the initial isotropic stress field, gives the following relation for the out-of-plane stress:

$$\sigma_z = \nu(\sigma_r + \sigma_t) + (1 - 2\nu)\sigma_0. \tag{13}$$

Despite the fact that a solution is available for the elastic problem in finite strains (e.g. Durban [19]), it cannot be expressed in closed form (except for the special case of $\nu = 0.5$). Nevertheless, in the case considered here (elastic ground), the deformations will be small anyway. Consequently, we can neglect the higher order terms in the Taylor series of Eqs. (8) and (9). The kinematic relations then simplify to

$$\varepsilon_r = du/dr, \tag{14}$$

$$\varepsilon_t = u/r, \tag{15}$$

which can be combined to yield the compatibility equation

$$\frac{d\varepsilon_t}{dr} + \frac{\varepsilon_t - \varepsilon_r}{r} = 0. \tag{16}$$

This equation in combination with the constitutive relations (10), (11), the equilibrium equation (7) and the boundary condition (5) leads to the following expression between the radial and tangential stresses:

$$\sigma_r + \zeta\sigma_t = (1 + \zeta)\sigma_0. \tag{17}$$

The stress and the displacement field around the cavity are given by the following equations (Yu and Rowe [10]):

$$\sigma_r = \sigma_0 - (\sigma_0 - \sigma_a)\left(\frac{a}{r}\right)^{\zeta+1}, \tag{18}$$

$$\sigma_t = \sigma_0 + \frac{\sigma_0 - \sigma_a}{\zeta}\left(\frac{a}{r}\right)^{\zeta+1}, \tag{19}$$

$$u = \frac{1 + \nu}{\zeta E}(\sigma_0 - \sigma_a)\left(\frac{a}{r}\right)^{\zeta+1} r. \tag{20}$$

At first glance, Eqs. (18)–(20) are identical with Kirsch's solution. This is because we neglected the higher order terms in the kinematic relationships (8) and (9). It should be noted, however, that in the present case (unlike Kirsch's solution), Eqs. (14), (15) and (18–20) refer to the deformed state.

DOI: 10.1002/nag

The expression for the construction of the GRC can be obtained from Eq. (20) by evaluating the displacement at the tunnel wall ($r=a$) and considering the displacement definition (Eq. (6)):

$$\frac{u_a}{a_0}=\left[1+\frac{\zeta E}{(1+\nu)(\sigma_0-\sigma_a)}\right]^{-1}. \tag{21}$$

Apparently, Eq. (21) gives almost the same results with the classic small strain elastic solution as long as $u_a/a_0<5\%$, which is mostly the case for the materials of interest (hard soils and soft/weak rocks) justifying further the use of linear elasticity. The reason behind implementing the above approximate finite strain approach in case of elastic response is that it is more compatible with the strain field in the plastic zone, where an exact finite strain formulation is considered (Section 5).

5. DERIVATION FOR ELASTOPLASTIC BEHAVIOUR

5.1. Cylindrical cavities without out-of-plane flow or spherical cavities

5.1.1. Introduction. Upon unloading, the ground behaviour remains purely elastic until the failure criterion is attained at the cavity wall. As the support pressure continues to diminish, the ground around the opening becomes more and more plastified, forming an increasingly thick plastic ring. The outer radius of the plastic ring will be denoted here by ρ_1 (Figure 3b).

For the two-dimensional case (i.e. a cross section of a cylindrical cavity under plane-strain conditions), it is assumed in the analysis of Section 5.1 that the axial stress is the intermediate principal stress. However, this does not always apply. A further decrease in the support pressure may lead to the violation of this condition (depending on the ground properties) and thus to the creation of a second inner plastic ring, where the plastic flow takes place both in the cross section under consideration and in the axial direction. This case, where the out-of-plane stress ceases to be the intermediate principal stress, is examined in Section 5.2.

The equations can be simplified considerably by applying Caquot's [20] transformation to all normal stresses σ (actually constituting a transformation from a cohesionless to a cohesive material, cf. also Anagnostou and Kovári [21]) and by normalizing the transformed stress by Young's modulus E:

$$\widetilde{\sigma}=\frac{1}{E}\left(\sigma+\frac{\sigma_D}{m-1}\right). \tag{22}$$

5.1.2. Ground response in the elastic zone. The stress state at the elastoplastic interface fulfills both the basic property of the elastic response (Eq. (17)) and the failure criterion (Eq. (1), with $\sigma_1=\sigma_t$ and $\sigma_3=\sigma_r$) which, using the aforementioned transformation (Eq. (22)), becomes

$$\widetilde{\sigma}_t=m\widetilde{\sigma}_r. \tag{23}$$

From Eqs. (17) and (23), we obtain the radial stress at the elastoplastic boundary:

$$\widetilde{\sigma}_{\rho 1}=\frac{\zeta+1}{\zeta m+1}\widetilde{\sigma}_0. \tag{24}$$

This relation is identical to the well-known one from the small strain formulation (cf., e.g., Panet [1]) owing to the negligence of higher order terms in the strain definitions during elastic response, which led to Eq. (17). Note that in case of elastoplastic behaviour even though the total strains may be large, the elastic strain components are small, allowing thus for the assumption of linear elasticity and implying that the large strains are induced by the plastic deformations. The stress $\sigma_{\rho 1}$ according to Eq. (24) also represents the critical support pressure, i.e. the support pressure at the onset of plastification. The ground behaviour is elastic if $\sigma_a\geq\sigma_{\rho 1}$ and elastoplastic if $\sigma_a<\sigma_{\rho 1}$.

For the outer elastic zone, the equations of Section 4 can be applied in order to obtain the stress and displacement fields. More specifically, by substituting the internal pressure σ_a by $\sigma_{\rho 1}$ and the cavity radius a by ρ_1 we obtain from Eqs. (18)–(20):

DOI: 10.1002/nag

$$\widetilde{\sigma}_r = \widetilde{\sigma}_0 - \left(\widetilde{\sigma}_0 - \widetilde{\sigma}_{\rho 1}\right)\left(\frac{\rho_1}{r}\right)^{\zeta+1}, \tag{25}$$

$$\widetilde{\sigma}_t = \widetilde{\sigma}_0 + \frac{\widetilde{\sigma}_0 - \widetilde{\sigma}_{\rho 1}}{\zeta}\left(\frac{\rho_1}{r}\right)^{\zeta+1}, \tag{26}$$

$$u = \frac{1+\nu}{\zeta}\left(\widetilde{\sigma}_0 - \widetilde{\sigma}_{\rho 1}\right)\left(\frac{\rho_1}{r}\right)^{\zeta+1} r. \tag{27}$$

Eq. (27) yields the radial displacement at $r=\rho_1$:

$$u_{\rho 1} = \frac{1+\nu}{\zeta}\left(\widetilde{\sigma}_0 - \widetilde{\sigma}_{\rho 1}\right)\rho_1. \tag{28}$$

Due to the continuity requirement for the radial displacement at the elastoplastic interface, Eq. (28) will serve later (in Section *5.1.4*) as a boundary condition for the integration of the differential equation governing the plastic zone.

5.1.3. Stress field in the plastic zone. The stress field inside the plastic region ($a \le r < \rho_1$) fulfils both the equilibrium condition (Eq. (7)) and the failure criterion (Eq. (23)). These two equations lead to an ordinary differential equation, whose solution for the boundary condition (4) reads as follows:

$$\widetilde{\sigma}_r = \widetilde{\sigma}_a\left(\frac{r}{a}\right)^{\zeta(m-1)}. \tag{29}$$

The current plastic radius ρ_1 can be determined from Eq. (29) taking into account the continuity of the radial stress at the elastoplastic interface and Eq. (24):

$$\frac{\rho_1}{a} = \left(\frac{\widetilde{\sigma}_{\rho 1}}{\widetilde{\sigma}_a}\right)^{\frac{1}{\zeta(m-1)}}. \tag{30}$$

Eqs. (29) and (30) are similar to the equations for the small strain analysis. However, it should be emphasized again that both the tunnel radius a and the coordinate r refer to the deformed configuration. This means that the stress field and the radius of the plastic zone cannot be determined a priori without knowledge of the displacements, in contrast to the infinitesimal strain formulation which leads to a statically determinate solution (cf., e.g., Panet [1]).

Note that the extent of plastification around the opening depends on the current tunnel radius (Eq. (30)), implying that it also depends on the dilatancy. Specifically, the higher the dilation angle (and thus the larger the wall convergences), the smaller the plastic zone.

5.1.4. Displacement field in the plastic zone. According to the flow theory of plasticity, the total strain rates (or increments since there is no time dependency) can be decomposed into elastic and plastic ones, while the incremental plastic strain components can be expressed by means of a flow rule, which in general may be non-associated. Assuming that the plastic potential is obtained from the MC failure surface after replacing the friction angle φ by the dilation angle ψ, where $0^\circ \le \psi \le \varphi$, it follows after some manipulation that

$$d\varepsilon_r^{PL} + \zeta\kappa d\varepsilon_t^{PL} = 0, \tag{31}$$

where

$$\kappa = \frac{1+\sin\psi}{1-\sin\psi}. \tag{32}$$

For the elastic strain components, the constitutive relations (10) and (11) can be used. (These equations are also valid for the plane-strain problem because the present section assumes that there is no out-of-plane plastic flow.) The adopted constitutive model assumes that the neither the elastic constants nor the yielding

DOI: 10.1002/nag

conditions are affected by the plastic flow. Integrating the resulting expression for the strain increments with respect to the initial condition (isotropic, uniform stress field σ_0), Eq. (31) gives

$$\varepsilon_r + \zeta\kappa\varepsilon_t = \omega_{11}(\widetilde{\sigma}_r - \widetilde{\sigma}_0) + \omega_{21}(\widetilde{\sigma}_t - \widetilde{\sigma}_0), \tag{33}$$

where

$$\omega_{11} = \frac{1+v}{1+(\zeta-1)v}[1-(2-\zeta)v-\zeta v\kappa], \tag{34}$$

$$\omega_{21} = \zeta\frac{1+v}{1+(\zeta-1)v}[\kappa(1-v)-v]. \tag{35}$$

In order to account for large deformations in the plastic zone, the exact definition of the logarithmic strains must be used. Therefore, Eq. (33) yields, with the aid of the kinematic relations (8) and (9) as well as Eqs. (23) and (29):

$$\ln\left[\left(1+\frac{du}{dr}\right)\left(1+\frac{u}{r}\right)^{\zeta\kappa}\right] = \ln(\Omega_{11}) + \Omega_{21}\left(\frac{r}{a}\right)^{\zeta(m-1)}, \tag{36}$$

where

$$\Omega_{11} = \exp[-(\omega_{11}+\omega_{21})\widetilde{\sigma}_0], \tag{37}$$

$$\Omega_{21} = (\omega_{11} + m\omega_{21})\widetilde{\sigma}_a. \tag{38}$$

Eq. (36) may be rewritten as

$$\frac{d\left[(u+r)^{\zeta\kappa+1}\right]}{dr} = (\zeta\kappa+1)\Omega_{11}r^{\zeta\kappa}\exp\left[\Omega_{21}\left(\frac{r}{a}\right)^{\zeta(m-1)}\right]. \tag{39}$$

Consequently, the problem has been converted from the solution of an ordinary differential equation to the computation of a definite integral (on the right side of Eq. (39)). After integration of Eq. (39) with respect to the Eulerian radial coordinate r over the region $[r, \rho_1]$ and considering the transformation

$$T(r) = \left(\frac{r}{a}\right)^{\zeta(m-1)}, \tag{40}$$

we obtain

$$\left(\frac{u+r}{a}\right)^{\zeta\kappa+1} = C_1 - \delta\cdot\Omega_{11}\cdot\int_{T(r)}^{T(\rho_1)} T^{\delta-1}\exp(\Omega_{21}T)dT, \tag{41}$$

where

$$\delta = \frac{\zeta\kappa+1}{\zeta(m-1)}, \tag{42}$$

$$C_1 = \left[1+\frac{1+v}{\zeta}\left(\widetilde{\sigma}_0 - \widetilde{\sigma}_{\rho 1}\right)\right]^{\zeta\kappa+1}\left(\frac{\widetilde{\sigma}_{\rho 1}}{\widetilde{\sigma}_a}\right)^{\delta}. \tag{43}$$

The constant C_1 has been derived taking into account the continuity of displacements at the elastoplastic boundary and taking account of Eq. (28). Representing the above definite integral as a function $f_1(x, y)$, where the independent variables x, y correspond to the lower and the upper integration bounds, respectively, we now have

DOI: 10.1002/nag

$$\frac{r_0}{a} = \left[C_1 - \delta \cdot \Omega_{11} \cdot f_1\left(T(r), \frac{\widetilde{\sigma}_{\rho 1}}{\widetilde{\sigma}_a}\right)\right]^{\frac{1}{\zeta\kappa+1}}. \tag{44}$$

One can readily verify that the coefficient Ω_{21} (Eq. (38)) is positive. This does not allow the definite integral under consideration to be represented in terms of the incomplete gamma function (in the field of real numbers). Therefore, following Yu and Houlsby [17], the expansion of the exponential function in the power series will be used in order to provide a direct closed-form expression for the function f_1:

$$\exp(\Omega_{21} T) = \sum_{n=0}^{\infty} \frac{(\Omega_{21} T)^n}{n!}, \tag{45}$$

which leads to the following infinite sum expression:

$$f_1(x, y) = \sum_{n=0}^{\infty} \frac{{\Omega_{21}}^n}{n!(n+\delta)} \left(y^{n+\delta} - x^{n+\delta}\right). \tag{46}$$

On account of the form of Eq. (44), an inverse procedure is necessary for the estimation of the displacement field inside the plastic region. Specifically, given the current position r of a material point, ensuring that $a < r < \rho_1$, its initial position r_0 is evaluated through Eq. (44) (and its corresponding displacement through Eq. (6)).

Moving one step further now in order to obtain the current radius of the cavity, the lower integration bound r is set equal to a and Eq. (44) produces:

$$\frac{a}{a_0} = \left[C_1 - \delta \cdot \Omega_{11} \cdot f_1\left(1, \frac{\widetilde{\sigma}_{\rho 1}}{\widetilde{\sigma}_a}\right)\right]^{-\frac{1}{\zeta\kappa+1}}. \tag{47}$$

The whole behaviour of the ground around a cylindrical or spherical opening can now be determined via closed-form analytical expressions which do not impose any restriction on the magnitude of the deformations.

5.1.5. Discussion. It would be instructive here to discuss the closed-form solution derived above with respect to existing studies which investigate the displacement field in similar cavity problems (either expansion or contraction) under finite deformations.

Chadwick [18], who was occupied with expanded spherical cavities in metals satisfying the Tresca model, suggested the numerical integration of the equation derived through the plastic flow rule, while in order to provide an explicit closed-form solution, he neglected the higher order terms of the logarithmic strains not only in the elastic zone (which is justifiable) but also in the plastic zone, where the deformations are inherently large. It should be noted that this approach results in the same relations with the infinitesimal strain formulation; however, there is a fundamental distinction between the material and spatial radial coordinates. Later, he used the MC model (still for the cavity expansion problem), but he did not determine the displacement field (Chadwick [22]).

Bigoni and Laudiero [16] also did not solve the differential equation of the cavity expansion problem analytically. They proposed an approximate closed-form solution by omitting the elastic deformations in the plastic zone, which means that the right side of Eq. (33) in the present paper vanishes.

Yu and Houlsby [17] presented the first exact closed-form solution to the cavity expansion problem by implementing the definition of the exponential function in power series (cf. Eq. (45)). As with all of the aforementioned authors, they followed a slightly different method, incorporating the definition of displacements (Eq. (6)) into the logarithmic strains (Eqs. (8) and (9)) and integrating after accounting for the appropriate transformations, which, however, is equivalent to the current process. On the other hand, Yu and Rowe [10], who investigated the corresponding cavity contraction problem for linearly elastic-perfectly plastic materials, resulted in Eq. (33), suggesting its numerical integration, whereas as Bigoni and Laudiero [16] neglected elastic deformations within the plastic region in order to provide an

DOI: 10.1002/nag

explicit expression for the characteristic line of the ground. As will be shown in Section 8, the error of this approximation can be significant.

5.2. Cylindrical cavities with out-of-plane flow

5.2.1. Overview of the ground response. The previous elastoplastic analysis concerning a cylindrical cavity ($\zeta = 1$) is based on the assumption that the axial stress is the intermediate principal stress. However, this condition may be violated during the unloading of the tunnel cross section depending on the ground properties and the in situ stress field. More specifically, with decreasing tunnel support pressure, the longitudinal stress decreases as well, but at a lower rate than the tangential stress inside the plastic zone. When the support pressure reaches a critical value (cf. Section *5.2.2*), the axial stress becomes equal to the tangential stress. Afterwards, they decrease at the same rate, i.e. they remain equal. At support pressures lower than the aforementioned critical value, an inner plastic zone with outer radius ρ_2 develops (Figure 3c, cf. Section *5.2.3*), where plastic flow also occurs in the axial direction. Section *5.2.4* contains the proof for this so-called edge plastic flow, while Section *5.2.5* derives the analytical solution for the displacement field.

5.2.2. Support pressure at the onset of out-of-plane plastic flow. At the interface of the two plastic zones ($r = \rho_2$), the following conditions apply: (i) the axial stress $\sigma_z = \sigma_t$; (ii) both stresses satisfy the failure criterion (Eq. (23)) as maximum principal stresses; and (iii) the elastic relation for the axial stress (Eq. (13)) is still valid. From these conditions, we obtain the radial stress at the interface of the two plastic regions ($r = \rho_2$):

$$\widetilde{\sigma}_{\rho 2} = \frac{1 - 2\nu}{m(1 - \nu) - \nu} \widetilde{\sigma}_0. \tag{48}$$

This stress also represents the support pressure at the onset of the out-of-plane plastic flow.

5.2.3. Stress field and radius of the inner plastic zone. The stress and displacement fields in the elastic region and in the outer plastic ring are still given by Eqs. (13) and (25–27), and Eqs. (13), (23), (29) and (44), respectively. The stress field in the entire plastic domain is calculated using the equilibrium condition (7) and the failure criterion (23); hence, the radial stress within the inner plastic zone is given by Eq. (29) and the radius ρ_1 is still obtained by Eq. (30), while the axial stress – as mentioned above and proved in the next section – is equal to the tangential one, i.e. $\sigma_z = \sigma_t$ with σ_t according to Eq. (23). On the other hand, the radius ρ_2 can be estimated via Eq. (29), by setting the radial stress at the interface equal to the critical stress value $\sigma_{\rho 2}$, resulting in

$$\frac{\rho_2}{a} = \left(\frac{\widetilde{\sigma}_{\rho 2}}{\widetilde{\sigma}_a} \right)^{\frac{1}{m-1}}. \tag{49}$$

5.2.4. Proof for the presence of edge plastic flow. At support pressures σ_a lower than the critical pressure $\sigma_{\rho 2}$, either the longitudinal stress (rather than the tangential stress) will become the major principal stress within the inner plastic ring, i.e. $\sigma_r < \sigma_t < \sigma_z$ (hereafter referred to as hypothesis 1); or these two stresses will remain equal, i.e. $\sigma_r < \sigma_t = \sigma_z$, and move on an edge of the pyramidal failure surface after MC (hypothesis 2).

Reed [15] has presented a rigorous proof for hypothesis 2 within the framework of small strains, applying the principle of reductio ad absurdum. More specifically, he compared the derivatives of the stresses at the interface of the two plastic rings, resulting in an inconsistency. A more direct and general proof (valid irrespective of the deformation formulation) is provided here, also applying the reductio ad absurdum.

Hence, let us assume the validity of hypothesis 1, i.e. that the out-of-plane stress is the major principal stress. Then,

$$\widetilde{\sigma}_t < \widetilde{\sigma}_z, \tag{50}$$

and according to the MC yield criterion,

DOI: 10.1002/nag

$$\widetilde{\sigma}_z = m\widetilde{\sigma}_r. \tag{51}$$

In addition, each material point that passes into the inner plastic zone (inner plastic zone meaning here the zone where $\sigma_r < \sigma_t < \sigma_z$) will further develop only elastic tangential strains because the tangential stress is – according to hypothesis 1 – the intermediate principal stress. The additional tangential strain, i.e. the strain that develops at the point under consideration after the inner zone reaches this point (or, in other words, the strain developing after the radial stress σ_r at the point under consideration drops below $\sigma_{\rho 2}$), is then given by Hooke's law:

$$\varepsilon_t - \varepsilon_t|_{\tilde{\sigma}_r=\tilde{\sigma}_{\rho 2}} = \widetilde{\sigma}_t - \widetilde{\sigma}_t|_{\tilde{\sigma}_r=\tilde{\sigma}_{\rho 2}} - \nu\Big(\widetilde{\sigma}_r - \widetilde{\sigma}_{\rho 2} + \widetilde{\sigma}_z - \widetilde{\sigma}_z|_{\tilde{\sigma}_r=\tilde{\sigma}_{\rho 2}}\Big). \tag{52}$$

Taking into account Eqs. (51) and (52) as well as that

$$\widetilde{\sigma}_t|_{\tilde{\sigma}_r=\tilde{\sigma}_{\rho 2}} = \widetilde{\sigma}_z|_{\tilde{\sigma}_r=\tilde{\sigma}_{\rho 2}} = m\widetilde{\sigma}_{\rho 2}, \tag{53}$$

the inequality (50) can be written as follows:

$$[m(1-\nu)-\nu]\big(\widetilde{\sigma}_r - \widetilde{\sigma}_{\rho 2}\big) > \varepsilon_t - \varepsilon_t|_{\tilde{\sigma}_r=\tilde{\sigma}_{\rho 2}}. \tag{54}$$

One can readily verify that the term on the left is always negative (because $m(1-\nu) > \nu$ and $\sigma_r < \sigma_{\rho 2}$), while the right side is always positive. Thus, Eq. (54) cannot be valid, which means that the leading hypothesis 1 (Eq. (50)) is false and that hypothesis 2 must apply instead.

5.2.5. Displacement field in the inner plastic zone. Analogously to Section *5.1.4*, the plastic flow rule shall be used to determine the displacements in the inner plastic ring. It should be pointed out that, as the problem allows for integration over the entire loading history, i.e. obtaining only the final state of the material response, the same results could be obtained using the deformation theory of plasticity (Papanastasiou and Durban [9], Chen and Han [23], Duncan Fama [24]). The implementation of Koiter's [25] rule, according to which the plastic strain increment is equal to a linear combination of the normal vectors of the two potential surfaces, results after some minor manipulation in

$$d\varepsilon_r^{PL} + \kappa d\varepsilon_t^{PL} + \kappa d\varepsilon_z^{PL} = 0. \tag{55}$$

Decomposing the total strain increments into elastic and plastic ones and taking into account the complete constitutive equations for linear elasticity (instead of Eqs. (10) and (11)), the plane-strain assumption (i.e. $d\varepsilon_z = 0$) and the fact that the axial stress is equal to the tangential one throughout the inner plastic ring (i.e. $\sigma_z = \sigma_t$), Eq. (55) can be integrated to yield

$$\varepsilon_r + \kappa\varepsilon_t = \omega_{12}(\widetilde{\sigma}_r - \widetilde{\sigma}_0) + \omega_{22}(\widetilde{\sigma}_t - \widetilde{\sigma}_0), \tag{56}$$

where

$$\omega_{12} = 1 - 2\nu\kappa, \tag{57}$$

$$\omega_{22} = 2[\kappa(1-\nu) - \nu]. \tag{58}$$

Recalling the logarithmic strains (Eqs. (8) and (9)), Eq. (56) can be converted into

$$\ln\left[\left(1+\frac{du}{dr}\right)\left(1+\frac{u}{r}\right)^{\kappa}\right] = \ln(\Omega_{12}) + \Omega_{22}\left(\frac{r}{a}\right)^{m-1}, \tag{59}$$

where

$$\Omega_{12} = \exp[-(\omega_{12}+\omega_{22})\widetilde{\sigma}_0], \tag{60}$$

$$\Omega_{22} = (\omega_{12} + m\omega_{22})\widetilde{\sigma}_a. \tag{61}$$

Integrating now over the region $[r, \rho_2]$, the relationship for estimating the Lagrangian coordinate of each material point with respect to the Eulerian one is obtained (similarly to Eq. (44)):

DOI: 10.1002/nag

$$\frac{r_0}{a}=\left[C_2-\delta\cdot\Omega_{12}\cdot f_2\left(T(r),\frac{\widetilde{\sigma}_{\rho 2}}{\widetilde{\sigma}_a}\right)\right]^{\frac{1}{\kappa+1}}, \tag{62}$$

where

$$C_2=C_1-\delta\cdot\Omega_{11}\cdot f_1\left(\frac{\widetilde{\sigma}_{\rho 2}}{\widetilde{\sigma}_a},\frac{\widetilde{\sigma}_{\rho 1}}{\widetilde{\sigma}_a}\right), \tag{63}$$

$$f_2(x,y)=\sum_{n=0}^{\infty}\frac{{\Omega_{22}}^n}{n!(n+\delta)}\left(y^{n+\delta}-x^{n+\delta}\right). \tag{64}$$

The constant C_2 has been obtained from Eq. (44), accounting for the continuity of displacements at the interface between the plastic zones. By evaluating Eq. (62) now at $r=a$, the current tunnel radius is deduced:

$$\frac{a}{a_0}=\left[C_2-\delta\cdot\Omega_{12}\cdot f_2\left(1,\frac{\widetilde{\sigma}_{\rho 2}}{\widetilde{\sigma}_a}\right)\right]^{-\frac{1}{\kappa+1}}. \tag{65}$$

6. SYNOPSIS OF THE FINITE STRAIN SOLUTIONS FOR THE GRC

The aforementioned expressions for the GRC (Eqs. (21), (47) and (65)) may be summarized in the following:

$$\frac{u_a}{a_0}=\begin{cases}\left[1+\dfrac{\zeta}{(1+\nu)(\widetilde{\sigma}_0-\widetilde{\sigma}_a)}\right]^{-1} & ,\quad \widetilde{\sigma}_{\rho 1}\le\widetilde{\sigma}_a;\\ 1-\left[C_1-\delta\cdot\Omega_{11}\cdot f_1\left(1,\dfrac{\widetilde{\sigma}_{\rho 1}}{\widetilde{\sigma}_a}\right)\right]^{-\frac{1}{\zeta\kappa+1}} & ,\quad \widetilde{\sigma}_{\rho 2}\overset{(\zeta=1)}{\le}\widetilde{\sigma}_a<\widetilde{\sigma}_{\rho 1};\\ 1-\left[C_2-\delta\cdot\Omega_{21}\cdot f_2\left(1,\dfrac{\widetilde{\sigma}_{\rho 2}}{\widetilde{\sigma}_a}\right)\right]^{-\frac{1}{\kappa+1}} & ,\quad \widetilde{\sigma}_a\overset{(\zeta=1)}{<}\widetilde{\sigma}_{\rho 2}.\end{cases} \tag{66}$$

For spherical cavities ($\zeta=2$), only the first two branches apply, while for cylindrical ones ($\zeta=1$), the third branch should be used additionally in order to account for the out-of-plane plastic flow, which leads to the formation of a second inner plastic ring. However, neglecting the out-of-plane flow does not greatly affect the results, as will be shown in Section 7. All the constants appearing in Eq. (66) in conjunction with the functions f_1, f_2 have been defined in the previous sections. It should be noted that the above infinite series (Eqs. (46) and (64)) converge rapidly and thus few terms suffice to obtain accurate results. Consequently, the derived solution for the GRC (as well as for the overall ground response around the cavity) can be implemented directly.

The transformation (22) has decreased the number of significant parameters of the problem. Thus, the normalized wall displacement can be expressed with respect to five instead of seven independent variables as:

$$\frac{u_a}{a_0\widetilde{\sigma}_0}=f\left(\frac{\widetilde{\sigma}_a}{\widetilde{\sigma}_0},\nu,\varphi,\psi,\widetilde{\sigma}_0\right). \tag{67}$$

Figure 4 presents normalized charts depicting the corresponding GRCs based on the proposed solution for various values of transformed initial stress $\widetilde{\sigma}_0$ and of the friction angle φ. The value of the Poisson's number ν was kept constant to 0.25, while the dilatancy angle ψ was taken equal to $\psi=\max(0^\circ,\ \varphi-20^\circ)$ (Vermeer and de Borst [26]). Such relatively small values of the dilatancy angle are typical for rocks in general and weak rocks in particular (Vogelhuber [27]).

The diagrams on the left apply to cylindrical openings ($\zeta=1$), whereas those on the right apply to spherical cavities ($\zeta=2$). It should be mentioned that the uppermost curves ($\widetilde{\sigma}_0\approx 0$) coincide with the small strain solution, in which the last right side term of Eq. (67) disappears (Anagnostou and Kovári [21]).

DOI: 10.1002/nag

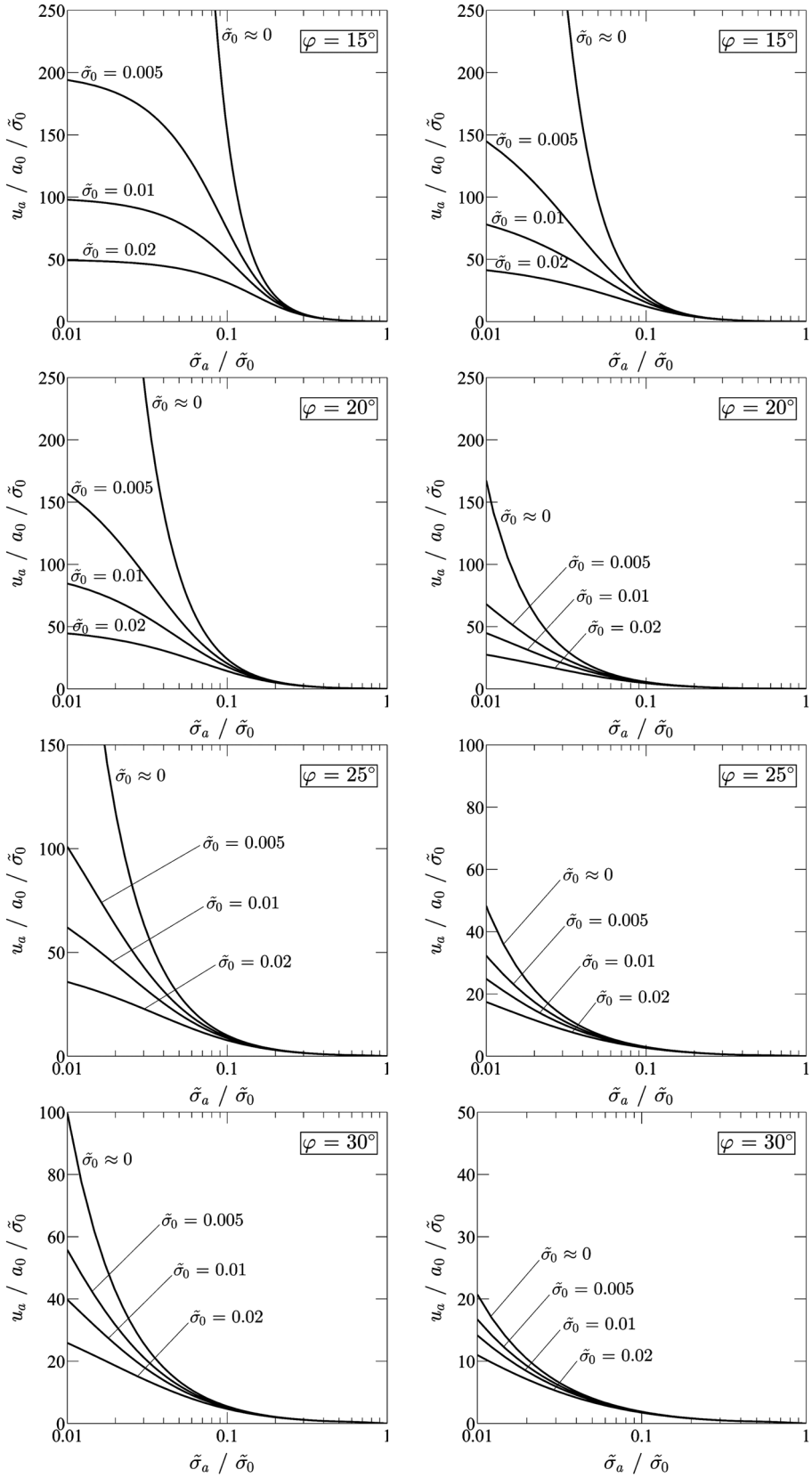

Figure 4. Ground response curves for several parameter sets, $\nu = 0.25$ and $\psi = \max\,(0°, \varphi - 20°)$ (left side diagrams: cylindrical cavity, right side diagrams: spherical cavity).

DOI: 10.1002/nag

As a result, the current charts also demonstrate the difference between the two formulations, for several parameter sets. Obviously, the poorer the quality of the ground, the higher the initial stress and the lower the support pressure, the larger will be the convergences, and thus the greater will be the error of infinitesimal deformation theory.

Furthermore, the expected higher stiffness of the spherical cavities owing to their three-dimensional arching effect is apparent in Figure 4. The diagrams for the spherical cavity problem can be used for a rough estimation of the axial deformation of the tunnel face in heavily squeezing ground (cf., e.g., Mair [14]).

7. INFLUENCE OF THE OUT-OF-PLANE PLASTIC FLOW FOR CYLINDRICAL CAVITIES

The influence of the out-of-plane plastic flow on the behaviour of unloaded cylindrical openings has been examined extensively in the past within the framework of small deformations, both analytically (e.g. Reed [15]) and numerically (e.g. Pan and Brown [28]). It has been shown that the tunnel wall convergences are affected slightly. A similar study is performed here. The error in the tunnel wall displacement arising from the negligence of the out-of-plane flow is estimated through

$$err_1 = \frac{u_a^{approx} - u_a^{Eq.(66)}}{u_a^{Eq.(66)}}, \tag{68}$$

where u_a^{approx} denotes the approximate solution (in particular, Eq. (66) is used omitting the third branch). Figure 5 plots the derived error for several material properties and $\widetilde{\sigma}_0 = 0.01$. Apparently, the negligence of plastic flow in the longitudinal direction slightly underestimates the predicted displacements in the case of extremely low values of ν. Therefore, it can be regarded as insignificant for practical purposes.

8. ERROR INDUCED BY NEGLECTING THE ELASTIC STRAINS IN THE PLASTIC ZONE

Yu and Rowe [10] have derived an approximate solution for the characteristic line of the rock by totally neglecting the elastic deformations within the plastic region. Thereafter, the right side of Eq. (36) becomes equal to unity, facilitating to a great extent the mathematical operations. The resulting error is defined analogously to Eq. (68) with u_a^{approx} corresponding to the approximate solution of Yu and Rowe [10]. Figure 6 demonstrates the calculated error for the cylindrical (left side diagrams) and spherical symmetry (right side diagrams), respectively, accounting for various parameter combinations ($\widetilde{\sigma}_0 = 0.01$). It can be observed that the error derived is significant at the practically relevant lower dilation angles. More specifically, the convergences may be underestimated up to 50%. The error diminishes for higher dilatancy, owing to the increase of plastic deformations. The

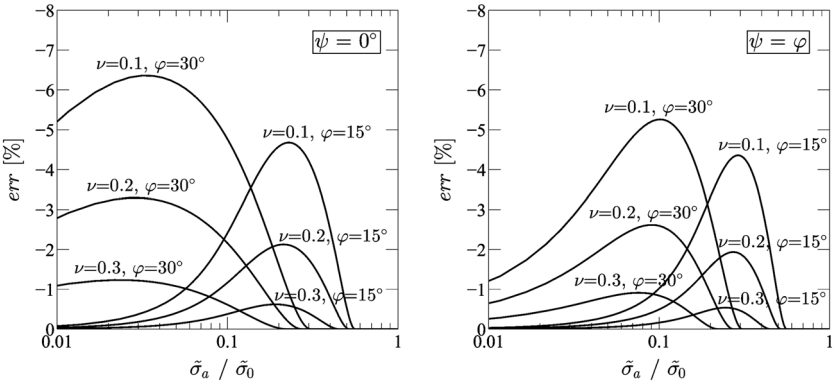

Figure 5. Error induced by neglecting the out-of-plane plastic flow in cylindrical openings under plane-strain conditions ($\widetilde{\sigma}_0 = 0.01$).

DOI: 10.1002/nag

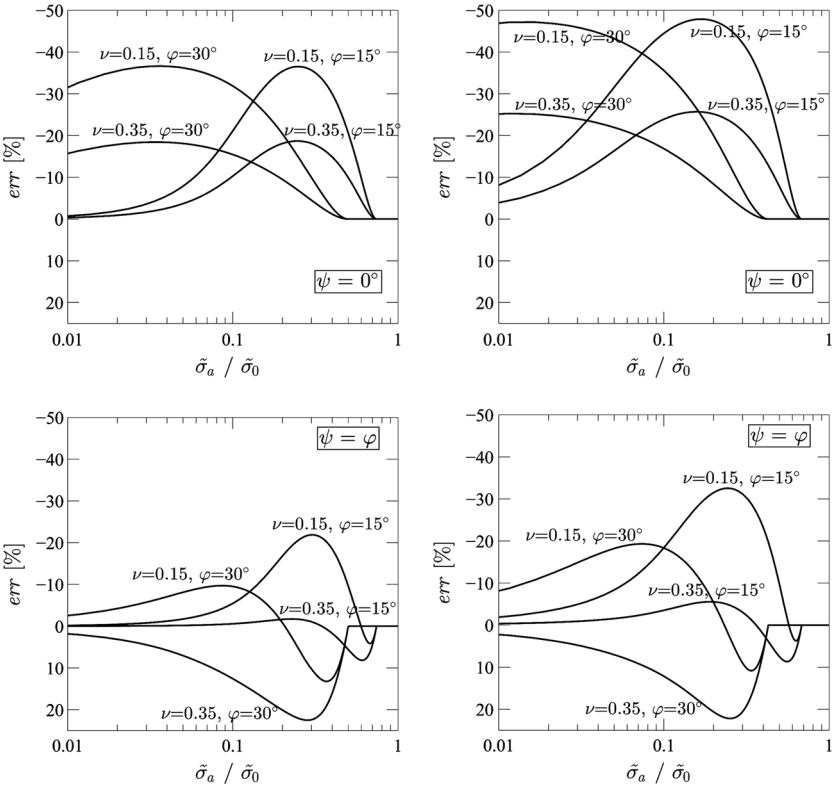

Figure 6. Error induced by neglecting the elastic deformations in the plastic zone ($\widetilde{\sigma}_0 = 0.01$, left side diagrams: cylindrical cavity, right side diagrams: spherical cavity).

two solutions coincide only in the case of $\psi = 0°$ and $v = 0.5$ (where both elastic and plastic volumetric strains equal zero). Finally, it is worth noting that the discrepancy from the accurate solution may be either positive or negative, depending on the support pressure (and thus on the extent of plastification).

9. APPLICATION EXAMPLE

The Sedrun section of the Gotthard Base tunnel in Switzerland is a typical case of heavily squeezing ground. It involves a distance of about 6 km of the 57 km long tunnel, passing through rocks of low strength and high deformability, the so-called kakiritic rocks, at a depth of 900 m ($\sigma_0 = 22.5$ MPa). The expectation of large deformations as a result of tunnel excavation led to a demanding design, including a circular tunnel cross section with full face excavation, uniform and systematic anchoring of the face as well as around the cross section, deliberate over-excavation up to 0.7 m in the least favourable rock zones (which corresponds in turn to an excavation radius of 6.5 m), steel arch linings with sliding connections and a closed ring of shotcrete lining in the region behind the face. A considerable reduction in the cross section beyond the planned values was, among others, one of the crucial hazard scenarios. Comprehensive descriptions of the project can be found elsewhere, cf. inter alia Kovári *et al.* [5].

Extensive laboratory tests on core samples from Sedrun were carried out at ETH Zurich (Vogelhuber [27]) and provided valuable information with respect to the mechanical properties of the rock. Accounting for these findings, Kovári *et al.* [5] proposed a geotechnical model corresponding to homogeneous and isotropic ground with the following material properties in the most unfavourable case: $E = 2000$ MPa, $c = 0.25$ MPa and $\varphi = 23°$, whereas the Poisson's ratio v and the dilation angle ψ can be taken equal to 0.25 and 3°, respectively (Vogelhuber [27]).

DOI: 10.1002/nag

Figure 7 shows the characteristic line according to both the finite strain and the small strain formulation, whereas Figure 8 illustrates the distribution of the stresses and of radial displacement in the radial direction for an unsupported opening ($\sigma_a = 0$ MPa).

The error of the small strain solution is very small up to convergence ratios u_a/a_0 of 10%, but at lower support pressures the small strain solution provides irrational results (convergences greater than the initial tunnel radius). The overestimation of the wall displacements at the support pressures of practical interest provided by yielding supports (several hundred kPa) is remarkable, highlighting the value of the finite strain solution.

Figures 7 and 8 additionally show – for the purpose of comparison only – the numerical results obtained for the same problem by using the finite element code Abaqus (Dassault Systèmes [29]). A simple axisymmetric strip with proper vertical restraints and a remote stress boundary condition is considered. Moreover, in order to ensure consistency of the computational assumptions, Clausen's [30] UMAT subroutine is used, utilizing the classic MC constitutive model, instead of the build-in subroutine of Abaqus, which uses a smoothened plastic potential. The finite element results lie in perfect agreement with the proposed closed-form solutions.

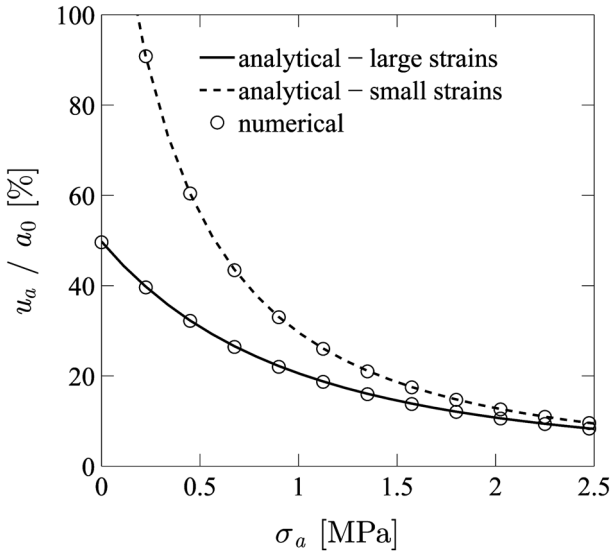

Figure 7. Characteristic lines for the Sedrun section of the Gotthard Base tunnel.

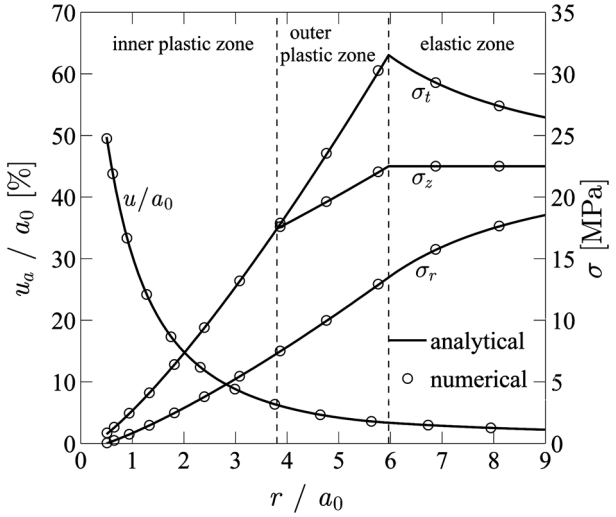

Figure 8. Radial distribution of stresses and of radial displacement (computational example for the Sedrun section of the Gotthard Base tunnel).

DOI: 10.1002/nag

10. CONCLUSIONS

We presented an exact closed-form finite strain solution for the unloading of cylindrical and spherical cavities. The motivation for this study was to investigate the response of the ground to tunnel excavation within a more rational framework in the case of weak rocks with high deformability. It was shown that the large deformation formulation may provide markedly lower convergences than the classic small strain solution for the GRC (for convergence ratios u_a/a_0 significantly greater than 10%). The solution presented can be used for convergence assessments in tunnelling, especially in the case of heavily squeezing ground.

Despite the existence nowadays of a wide variety of sophisticated computational tools, which allow for detailed numerical analyses of the expected ground response simulating the exact geotechnical profile as well as the successive excavation and support installation steps, closed-form analytical solutions are still valuable. Apart from a deeper insight into the significance of the several parameters involved in the problem, they can also serve as a benchmark for numerical procedures that account for material and geometric nonlinearities.

NOTATION

a_0, a	initial and current radius of the cavity
c	cohesion
C_1, C_2	integration constants
E	elastic (Young's) modulus
err	error estimations
f_1, f_2	functions of two variables
f	an arbitrary function
m	function of friction angle
n	index of infinite series
r_0, r	initial and current radius of a material point
T	transformation function
u	radial displacement of a material point
u_a	radial displacement at the cavity wall
x, y	auxiliary variables
δ	function of the material constants
ε_r	radial strain
ε_t	tangential strain
ε_z	out-of-plane (or axial or longitudinal) strain (for $\zeta = 1$)
ε_r^{EL}, ε_t^{EL}, ε_z^{EL}	elastic strain components
ε_r^{PL}, ε_t^{PL}, ε_z^{PL}	plastic strain components
ζ	variable that indicates the type of cavity ($\zeta = 1$ cylindrical, $\zeta = 2$ spherical)
κ	function of dilation angle
ν	Poisson's ratio
ρ_1	current radius of the plastic zone
ρ_2	current radius of the inner plastic zone (for $\zeta = 1$)
σ	normal stress
$\widetilde{\sigma}$	transformed normal stress
σ_r	radial stress
σ_t	tangential stress
σ_z	out-of-plane (or axial or longitudinal) stress (for $\zeta = 1$)
σ_0	in situ isotropic stress
σ_a	cavity support pressure
$\sigma_{\rho 1}$	radial stress at $r = \rho_1$
$\sigma_{\rho 2}$	radial stress at $r = \rho_2$ (for $\zeta = 1$)
σ_D	uniaxial compressive strength

DOI: 10.1002/nag

φ	friction angle
ψ	dilation angle
ω_{11}, ω_{21}	functions of the material constants
ω_{12}, ω_{22}	functions of the material constants (for $\zeta = 1$)
Ω_{11}, Ω_{12}	functions of the material constants and the in situ stress
Ω_{21}, Ω_{22}	functions of the material constants and the support pressure

REFERENCES

1. Panet M. Le calcul des tunnels par la méthode convergence-confinement. Presses de l'École Nationale des Ponts et Chaussées: Paris, 1995.
2. Brown ET, Bray JW, Ladanyi B, Hoek E. Ground response curves for rock tunnels. *ASCE Journal of Geotechnical Engineering* 1983; **109**(1):15–39.
3. Yu HS. Cavity Expansion Methods in Geomechanics. Kluwer Academic Publishers: Dordrecht, 2000.
4. Alonso E, Alejano LR, Varas F, Fdez-Manín G, Carranza-Torres C. Ground response curves for rock masses exhibiting strain-softening behaviour. *International Journal for Numerical and Analytical Methods in Geomechanics* 2003; **27**:1153–1185.
5. Kovári K, Amberg F, Ehrbar H. Mastering of squeezing rock in the Gotthard Base. *World Tunnelling* 2000; **13**(5):234–238.
6. Kovári K. Tunnelbau in druckhaftem Gebirge – Tunnelling in squeezing rock. *Tunnel* 1998; **5**:12–31.
7. Hoek E. Big tunnels in bad rock (The thirty-sixth Karl Terzaghi lecture). *ASCE Journal of Geotechnical and Geoenvironmental Engineering* 2001; **127**(9):726–740.
8. Barla G. Tunnelling under squeezing rock conditions. Tunnelling Mechanics: Eurosummerschool, Innsbruck, 2001 – Advances in Geotechnical Engineering and Tunnelling, Kolymbas D (ed.). Logos Verlag: Berlin, 2002; 169–268.
9. Papanastasiou P, Durban D. Elastoplastic analysis of cylindrical cavity problems in geomaterials. *International Journal for Numerical and Analytical Methods in Geomechanics* 1997; **21**:133–149.
10. Yu HS, Rowe RK. Plasticity solutions for soil behaviour around contracting cavities and tunnels. *International Journal for Numerical and Analytical Methods in Geomechanics* 1999; **23**:1245–1279.
11. Chen SL, Abousleiman YN. Exact drained solution for cylindrical cavity expansion in modified Cam Clay soil. *Géotechnique* 2012; **63**(6):510–517.
12. Egger P. Deformations at the face of the heading and determination of the cohesion of the rock mass. *Underground Space* 1980; **4**(5):313–318.
13. Labiouse V. Numerical and analytical modelling of a new gallery in the Boom Clay formation. Numerical Models in Geomechanics, Pietruszczak and Pande (eds.). Balkema: Rotterdam, 1997; 489–494.
14. Mair RJ. Tunnelling and geotechnics: new horizons. *Géotechnique* 2008; **58**(9):695–736.
15. Reed MB. The influence of out-of-plane stress on a plane strain problem in rock mechanics. *International Journal for Numerical and Analytical Methods in Geomechanics* 1988; **12**:173–181.
16. Bigoni D, Laudiero F. The quasi-static finite cavity expansion in a non-standard elasto-plastic medium. *International Journal of Mechanical Sciences* 1989; **31**(11):825–837.
17. Yu HS, Houlsby GT. Finite cavity expansion in dilatant soils: loading analysis. *Géotechnique* 1991; **41**(2):173–183.
18. Chadwick P. The quasi-static expansion of a spherical cavity in metals and ideal soils. *Quarterly Journal of Mechanics and Applied Mathematics* 1959; **12**(1):52–71.
19. Durban D. A finite-strain axially symmetric solution for elastic tubes. *International Journal of Solids and Structures* 1988; **24**(7):675–682.
20. Caquot A. Equilibre des massifs a frottemeni interne. Gauthier-Villars: Paris, France, 1934.
21. Anagnostou G, Kovári K. Significant parameters in elastoplastic analysis of underground openings. *ASCE Journal of Geotechnical Engineering* 1993; **119**(3):401–419.
22. Chadwick P. Propagation of spherical plastic-elastic disturbances from an expanded cavity. *Quarterly Journal of Mechanics and Applied Mathematics* 1962; **15**(3):349–376.
23. Chen WF, Han DJ. Plasticity for Structural Engineers. Springer-Verlag: New York, 1988.
24. Duncan Fama ME. Numerical modeling of yield zones in weak rock. Comprehensive Rock Engineering – Volume 2: Analysis and Design Methods, Hudson JA *et al*. (eds.). Pergamon Press: Oxford, 1993; 49–75.
25. Koiter WT. Stress-strain relations, uniqueness and variational theorems for elastic-plastic materials with a singular yield surface. *Quarterly of Applied Mathematics* 1953; **11**(3):350–354.
26. Vermeer PA, de Borst R. Non-associated plasticity for soils, concrete and rock. *Heron* 1984; **29**(3):1–64.
27. Vogelhuber M. Der Einfluss des Porenwasserdrucks auf das mechanische Verhalten kakiritisierter Gesteine. Dissertation Nr. 17079, Institut für Geotechnik, ETH Zürich, 2007.
28. Pan X-D, Brown ET. Influence of axial stress and dilatancy on rock tunnel stability. *ASCE Journal of Geotechnical Engineering* 1996; **122**(2):139–146.
29. Dassault Systèmes. Abaqus 6.11 – Theory Manual and Analysis User's Manual, 2011.
30. Clausen J. Efficient non-linear finite element implementation of elasto-plasticity for geotechnical problems. Ph.D. thesis, Esbjerg Institute of Technology, Aalborg University, 2007.

DOI: 10.1002/nag